INTERFACE THERMAL BEHAVIOUR OF COMPOSITE SECTIONS WITH THE FINITE ELEMENT METHOD—(ECCM –ECFD 2018 CONFERENCE)

Zheng Cui[1] and Y T Feng[1]

[1] Zienkiewicz Centre for Computational Engineering,
College of Engineering Swansea University, Bay Campus, SA1 8EN, United Kingdom
zheng.cui@swansea.ac.uk

Key words: Thermal affect; Composite sections; Interface behaviour

Abstract. This papaer conducts the interface thermal behaviour of both Concrete filled steel tube (CFT) and Concrete filled double skins steel tube (CFDST) sections with the Finite Element Method. One unheated section will be simulated for comparison. The contact thermal property and material thermal properties will be involved in this paper. Based on parametric analysis outcomes, the influence of the heating time, interface types and types of composite sections on the mechanical behaviour are considered. Test results indicate that the time length of fire exposure has a significant impact on the interface between steel tubes and concrete cores; also, the mechanical behaviour of CFT sections and CFDST sections are quite different under a fire condition. Further compared results of composite sections under a fire condition are investigated in this paper.

1 Introduction

Concrete filled steel tube(CFT) and concrete filled double skin steel tube(CFDST) are called composite construction sections, which contains steel tubes and concrete cores. Composite sections have been widely used as columns, especially in high-rise building structures and bridge piers. Compared with ordinary structural sections, they have many advantages. Firstly, the local buckling of the steel tube is delayed due to the restraining effect of the concrete. And the strength of the concrete is increased by the confining effect provided by the steel tube. Secondly, many research work have proved that they are more stable and can carry more loads than reinforced concrete. Therefore, the cross-sectional area is less needed.

After the "911 attack" event, fire resistance is the major factor that needs to be considered in composite structures. During a fire condition, the individual strength of steel and concrete parts will reduce dramatically. However, the interface behaviour under a fire condition is main concern. Tao et al. [7] illustrates that the bond strength of the CFT section generally decreases after exposing to fire 90 mins, and the strength can increase when the fire exposure time is 180 mins. Because after exposing to fire 180 mins, the concrete starts to dilate under a axial compression. In this way, the damaged concrete

increases the contact compression to the steel tube. Roeder et al. [9] establishes that the concrete shrinkage is harmful to the bond stress capacity, also the column size of the CFT section will affect the bond strength. Song et al. [6] indicates that the bond strength is negligible for all CFDST specimens with normal interface in the fire condition. As a gap is produced during fire exposure, the bond strength of CFDST specimens decreases by dropping the friction at the interface. Furthermore, the post-fire bond strength of CFDST specimens increases with the increasing of the axial loading ratio, because of the concrete dilation and local buckling of the steel tube.

Composite sections are caged the concrete core inside of the steel tube. Therefore, steel tubes protect and enhance the concrete core. There are challenges that arise when working with fire conditions. In particular, it is difficult for experiments to learn the information at the interface during a fire condition. Hence, a sufficient Finite Element Model has huge advantages. Such model should be capable of simulating the non-linear performance, large deformation and the corresponding results of composite sections.

This paper is forced on the thermal effect at the interface of composite sections under compression with a fire condition. Meanwhile, the confinement effect and interface behaviour were investigated in this paper. In order to achieve this goal, the contact thermal modelling and material thermal modelling will be discussed. A typical load versus displacement curve and displacement separation figures at interface will be used to illustrate the bond behaviour at the interface.

2 Theoretical basis

2.1 Interface Thermal Modelling

A heat treatment of a composite section is the process of the heat energy transmit from the external surface of the outer tube into the external surface of the inner tube. The interface thermal simulation has been applied to predict the fire behaviour of composite sections. Thermal contact properties including 3 parts: thermal conductance, radiation and heat generation. The Fully coupled thermal-stress analysis has been chosen. The temperatures are integrated using a backward difference scheme, and the non-linear coupled system is solved using Newton's method. An exact implementation of Newton's method is chosen for this simulation, and it is illustrated below.

$$
\begin{bmatrix} K_{uu} & K_{u\theta} \\ K_{\theta u} & K_{\theta\theta} \end{bmatrix} \begin{Bmatrix} \triangle u \\ \triangle \theta \end{Bmatrix} = \begin{Bmatrix} R_u \\ R_\theta \end{Bmatrix} \tag{1}
$$

where u and θ are the respective corrections to the incremental displacement and temperature, K_{ij} are sub-matrices of fully coupled Jacobian matrix, and R_u and R_θ are the mechanical and thermal residual vectors, respectively.

The use of the unsymmetrical matrix storage and solution scheme is required to solve this equation. However, due to calculation efficiency, the thermal and mechanical steps will be simulated separately. The mechanical step is based on the result of thermal step. The detailed information will be explained later.

2.1.1 Thermal Conductance between surfaces

Thermal conductance occurs at the interface of the composite section while the steel tube and the concrete core is in contact. An air gap may be produced at the interface when the section is exposed to fire. Because the value of thermal expansion for steel is much higher than that of concrete. Therefore, the expansion effect for steel is much greater. The conductive heat transfer between the contact surfaces is assumed to be defined by

$$q = k(\theta_A - \theta_B) \tag{2}$$

where q is the heat flux per unit area crossing the interface from point A on one surface to point B on another surface. θ_A and θ_B is the temperature of the corresponding point on surfaces, k is the gap conductance. Point A is one node on the slave surface and point B is another node on the master surface contacting the slave node. In this paper, surfaces from steel tubes are master surface and surfaces from concrete cores are slave surfaces. The master surfaces may penetrate through the slave surfaces.

The value of k can be defined directly as follow.

$$k = k(\overline{\theta}, d, p, \overline{|\dot{m}|}, \overline{f_\gamma}) \tag{3}$$

it is in a relationship with the average temperature of the surface $\overline{\theta}$, clearance between the contact surfaces d, the average of the mass flow rate $\overline{|\dot{m}|}$ and any predefined field variables at A and B $\overline{f_\gamma}$.

2.1.2 Modelling radiation between surfaces

The radiative heat energy is assumed that it transfers between closely spaced contact surfaces and it occurs in the direction of the normal between two surfaces. while modelling the interface, using surface-based contact discretization, the normal direction corresponds to the master surface normal.

Radiative heat transfer is defined as a function of clearance between the surfaces. The formulation is described that the monochromatic emissivity of the body is independent of the wavelength of propagation of the radiation. Only unidirectional diffused reflection is considered. Attenuation of the radiation in the cavity medium is not considered. Using those assumptions together with the assumption of isothermal and is emissive cavity facets, the equation for radiation flux per unit area q_j^c into a cavity facet j can be written as

$$\sum_j (\delta_{ij} + (\epsilon_j - 1)F_{ij})\frac{q_j^c}{\epsilon_j} = \sigma \sum_j F_{ij}((\theta_j - \theta^Z)^4 - (\theta_i - \theta^Z)^4) \tag{4}$$

where ϵ_j is the emissivity of facet j. σ is the Stefan-Boltzmann constant. F_{ij} is the geometrical viewfactor matrix. θ_i, θ_j are the temperatures of facets i, j. θ^Z is the value of absolute zero on the temperature scale being used. and δ_{ij} is the Kronecker delta.

2.1.3 Modelling heat generation

In fully coupled temperature-displacement simulations, heat generation due to the dissipation of energy created by the mechanical interaction of contacting surfaces. The main source of the heat is frictional sliding. All of the dissipated energy as heat will be released between the surfaces and distributes it equally between the two interacting surfaces. The fraction of dissipated energy can be converted into heat η and the weighting factor f for distribution of the heat between the interacting surfaces. In coupled thermal-mechanical surface interactions, the rate of frictional energy dissipation is given by

$$P_{fr} = \tau \cdot \dot{\gamma} \tag{5}$$

where τ is the frictional stress and $\dot{\gamma}$ is the slip rate.

The amount of this energy released as heat on each surface is assumed to be

$$q_A = f\eta P_{fr} \quad \text{and} \quad q_B = (1-f)\eta P_{fr} \tag{6}$$

where q_A and q_B are the heat flux into the slave and master surfaces, respectively.

2.2 Material Modelling

2.2.1 Steel Section

The classical plasticity model for steel is standard von Mises model failure surface with associated flow rule. Von Mises model is used to determine if a give material will yield or fracture. It is mostly used for ductile materials such as steel. Von Mises model states that if the von Mises stress of a material under a loading is equal or greater than the yield limit of the same material under a simple tension, then the material will yield. In the inequality form, the criterion may be put as

$$\sigma_{VM} \leq \sigma_Y \tag{7}$$

The von Mises stress σ_{VM} is given by

$$\sigma_{VM} = \sqrt{I_1^2 - 3I_2} \tag{8}$$

Then Eq. 8 can be expressed as follow

$$\sigma_{VM} = \frac{1}{2}\sqrt{(\sigma_1 - \sigma_2)^2 + (\sigma_2 - \sigma_3)^2 + (\sigma_3 - \sigma_1)^2} \tag{9}$$

The response of the steel tube is modelled by an elastic-perfectly-plastic theory with an associated flow rule. When the stress value is inside the stress yield surface, the behaviour of the steel tube is linearly elastic. Otherwise, the behaviour of the steel tube becomes perfectly plastic. Thus, the steel tube is assumed to fail and cannot resist any further loading.

2.2.2 Concrete Section

The Drucker-Prager failure criterion is a three-dimensional pressure-dependent model to estimate the stress state at which the concrete reaches its ultimate strength. The criterion is based on the assumption that the octahedral shear stress at failure depends linearly on the octahedral stress through material constants.

The Drucker-Prager failure criterion was established as a smooth version of the Mohr-Coulomb criterion. It can be expressed as:

$$\sqrt{J_2} = \lambda I_1' + \kappa \tag{10}$$

where the constants λ and κ are material constants. I_1' is the first invariant of the Cauchy stress and J_2 is the second invariant of the deviatoric part of the Cauchy stress.

The governing equation of the Drucker-Prager criterion, Eq. 10, illustrates a right-circular cone in the stress space when $\lambda > 0$, or a right circular cylinder when $\lambda = 0$. Hence, the intersection with the π-plane is a circle, as shown in Figure 1.

Since the Drucker-Prager yield surface is a smooth version of the Mohr-Coulomb yield surface, it is often expressed in terms of the cohesion(c) and the angle of internal friction(ϕ) that are used to describe the Mohr-Coulomb yield surface. If we assume that the Drucker-Prager yield surface circumscribes the Mohr-Coulomb yield surface, then the expression for λ and κ are

$$\lambda = \frac{2sin\phi}{\sqrt{3}(3 - sin\phi)} \qquad \kappa = \frac{6ccos\phi}{\sqrt{3}(3 - sin\phi)}$$

Han [5] found that the concrete core for CFDST sections has the similar failure performs compared with that for CFT sections. Therefore, the uni-axial stress-strain relation for steel and concrete in CFT sections has been used for the analysis of CFDST sections.
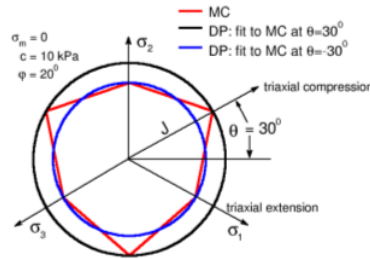

Figure 1: The inner and outer cones of the Drucker-Prager criterion match with the Mohr-Coulomb criterion

2.2.3 Material Thermal Modelling

The temperature field analysis bases on the thermal property of steel and concrete, such as, thermal conductivity, specific heat and thermal expansion. Thermal conductivity is the process of heat energy transfer from the hot to the cold part while they are contacted

$(W/m \cdot °C)$. Specific heat is the amount of heat energy per unite mass required to raise the temperature by one degree Celsius $(J/m^3 \cdot °C)$. And the thermal expansion refers to a fractional change in size of a material in response to a change in temperature $(W/m \cdot °C)$. Xu[**?**] has illustrated those properties of steel and concrete.
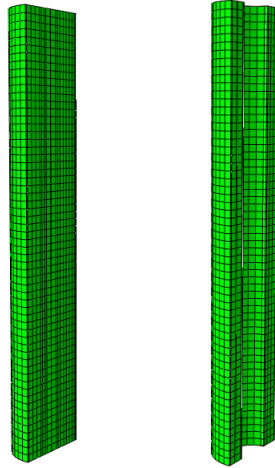
1. uniform distributed loading placed at the centre of the top surface
2. fully fixed at the centre point, and release x and y directions on the bottom surface

Figure 2: Finite Element meshing of CFT and CFDST models

3   Procedure of analysis

3.1   Finite Element Modelling

In this simulation, a numerical program will involve the heat transfer through the interface and influence of elevated temperature on the mechanical behaviour of composite sections. The heat transfer process can be simulated by using the numerical method, that are spatial discretization, time integration and solution for non-linear equations. A sequentially-coupled thermal-stress analysis has been applied to study the mechanical behaviour of composite columns exposed to fire conditions. The procedure will simulate the heat transfer step first. And then the temperature information will be imported into the mechanical step to calculate the structural response at different temperature levels. In order to transfer the accurate information of the nodal temperature from the heat transfer into the mechanical model, the mesh, interaction and nodal numbering are identical.

In the heat transfer step, the 20-node quadratic heat transfer brick (DC3D20) was chosen for concrete cores and steel tubes. And an 8-node linear brick, reduced integration 3D solid element(C3D8R) was used for concrete cores and steel tubes during the mechanical analysis step. For both steps, the mesh sizes are chosen to be 0.1 for steel tube and concrete core. The finite element mesh will be shown in the Figure 2.

Material properties are required in this analysis, which generally include elastic, plastic mechanical properties and thermal properties. Most of the mechanical properties are

temperature-dependent with elevated temperature. Young's modulus and Poisson's ratio are the fundamental factors associating with the mechanical properties. Li [11] and Ma et al. [10] have introduce the thermal properties of steel and concrete, respectively.

The applied fire condition on the external surface of the steel tube is the standard fire condition are defined by the ISO 834 fire condition [2], which specimens of constructions are subjected to. This curve is based on the burning rate of the materials found in general building materials and contents. The temperature development of the fire condition is described by following equation:

$$T = 20 + 345 \times log_{10}(\frac{2t}{15} + 1) \tag{11}$$

where t is the heating time in second, T is the temperature. Table 1 shows the information of the heating time, the corresponding unit is second. From the equation above, the corresponding temperature of 0, 3000 and 6000 seconds heating time are 20, 918 and 1021°C, respectively.

The interaction behaviour of steel tubes and concrete cores were simulated by the interface property. The contact surfaces between steel tubes and concrete cores are defined as contact pairs. There are two types of interfaces that are defined. One is defined as bonded interface. The mechanical property of the interaction will be defined in the tangential and normal behaviours. The normal behaviour will choose "Hard" as contact for pressure-overclosure. The cohesive properties(K_{nn}, K_{ss} and K_{tt}) are equal to $1 \times 10^{10} Pa$. and the damage coefficient (Normal, Shear-1 and Shear-2) will be $1 \times 10^{5} Pa$. Another one is nonbonded interface. It is simply no cohesive and damage properties at the interface contact. The section properties are shown in Table 1. Furthermore, the thermal conductance of contact surfaces need to be defined as clearance dependency for both types. When two surfaces are contacted, the conductance is 1000. If they are separated, which is the clearance distance is $0.01m$, the conductance is 0.

Table 1: Section Properties

CFT sections		CFDST sections	
Heating time(s)	Interface types	Heating time(s)	Interface types
0	Bonded interface	0	Bonded interface
3000	Bonded interface	3000	Bonded interface
3000	Nonbonded interface	3000	Nonbonded interface
6000	Bonded interface	6000	Bonded interface

The boundary conditions has shown in the Figure 2. Apart from the heat treatment at the external surface, another thermal boundary condition needs to be considered during this simulation. The external surface of the CFDST section can radiate in the air gap while the temperature is increasing. It will influence the temperature of the external surface. However, firstly, the cross-sectional shape of the CFDST section are symmetrical. Secondly, a part of the heating energy will transmit into the air to rise the air temperature

up. But for a complete CFDST section, the air at the middle is limited. Therefore, the heat loss at the inner surface can be ignored. Hence, the boundary condition at the inner surface of CFDST sections is simulated as no heat energy exchange with the external environment. Furthermore, only the external fire condition is considered, eg, the fire condition. Therefore, the radiation and heat generation aren't considered in this simulation.

3.2 Results

CFT sections and CFDST sections has different appearances after heated followed by the temperature pattern of Equation 11. Figures 3 (a) and (b) show that the temperature distribution on the top surface of CFT sections under the heating time of 3000 seconds and 6000 seconds, respectively. The colour pattern indicates the value of temperature. The temperature of outer tube for 6000s section is higher than that for 3000s section. As the temperature propagate into the concrete core, the temperature drops down. Figures 3 (c) and (d) show that the temperature distribution on the top surface of CFDST sections under the heating time of 3000 seconds and 6000 seconds, respectively.

(a) CFT section with 3000s heating time

(b) CFT section with 6000s heating time

(c) CFDST section with 3000s heating time

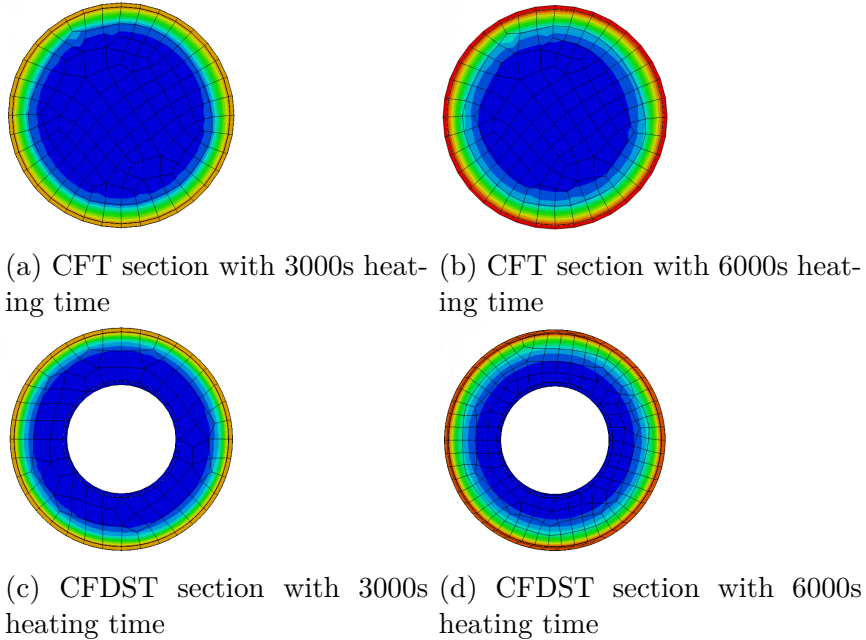(d) CFDST section with 6000s heating time

Figure 3: Temperature distribution of CFT sections

Due to the thermal expansion law, steel sections has larger expansion ratio compared with that of concrete sections. After increasing the temperature, a gap will be produced at the external interface of CFT and CFDST sections, thus the outer tube will provide less confinement to the concrete core during the fire exposure. However, at the internal interface of CFDST sections, the inner steel tube will produce an expansion pressure acting on the internal surface of the concrete core. Therefore, the confinement effect will improve at the inner interface of CFDST sections.
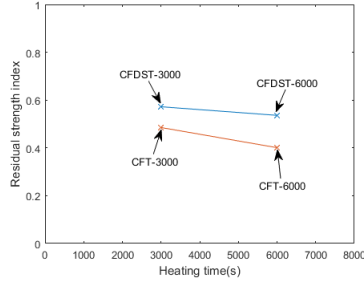
Figure 4: Residual strength index figure

3.2.1 Residual Strength

Steel and concrete sections are commonly known that they will lose amount of their strength during a fire condition, which is based on the temperature level. According to Han [8], for convenience of analysis, residual strength index is defined to quantify the strength of the composite section after exposure to fire condition. It is expressed as

$$RSI = \frac{N_u(t)}{N_u}$$

where $N_u(t)$ is the residual strength corresponding to the fire duration time t of the composite section, and N_u is the ultimate strength of the composite section at ambient temperature.

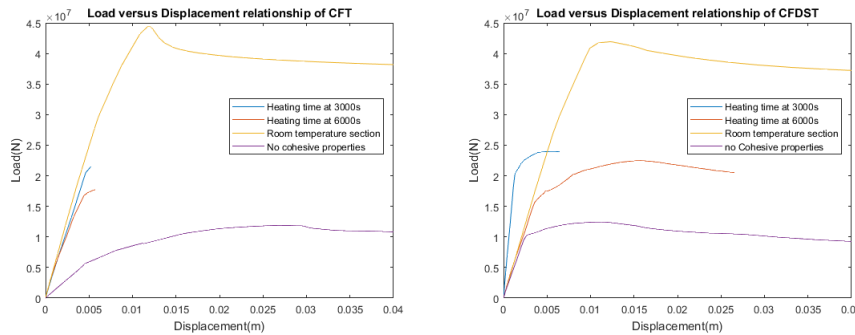Figure 4 shows Residual strength index of composite sections with different temperatures.

Figure 5: load versus displacement relationship of CFT and CFDST specimens

In the figure, the Residual strength of CFDST sections have better performances compared with CFT sections. A concerned test results of the simulation displayed a pleasant phenomenon. The unfilled tube has played an important role during the exposure of the fire condition. Even through steel tubes and concrete cores will lose their own strength during a fire condition, the inner tube will maintain most of the strength. Because the concrete core will absorb most of the heat energy. Hence, according to Figure 5, the elastic modulus of CFDST sections are significantly greater than that of CFT sections after exposure to fire condition.

9

3.3   Influence of different parameters

3.3.1   Effect of fire exposure

Obviously, the fire exposure could have a great impact on the cohesive bond strength at the interface between steel tubes and concrete cores. Moreover, it can cause the volume change and the shape change of steel tubes and concrete cores.

The compression versus displacement of CFT and CFDST sections undergo different heating times are shown in Figure 5. It can be found that the maximum loading is much greater for CFT and CFDST sections under room temperature. The slope of the initial curve of the 3000s heating section is greater than that of 6000s heating sections for both composite sections. However, the maximum loading dropped significantly from room temperature to 3000s heating time.

Figure 6 shows the displacement separation at the interface. Top figures are shown the thermal effect of CFT sections with different interface properties. The displacement changed a lot at the edge of top and bottom surfaces for nonbonded section. The external surface of the steel tube had massive movement near the loading surface (top surface), which means that the steel losses its strength during the simulation. As the temperature has risen. Similarly, for CFDST sections, the displacement shift at the interface is much larger for nonbonded section.

3.3.2   Effect of Composite section types

According to Zhao [3], the outer tube has similar behaviour with the tube of CFT sections. However, the inner tube will have similar behaviours with unfilled steel tubes. In general, the inner tube will have a weak performance compared with outer tube at the room temperature condition [4]. Figure 5 shows that the maximum loading of the room temperature section has similar values. When the heating time increases to 3000s, the maximum loading of CFDST sections is higher than that of CFT sections. Due to the confinement affect at the inner interface, the slope of the load-displacement curve of CFDST sections is greater than that of CFT sections. After heating time increased to 6000s, as the result of thermal expansion, the confinement affect at the inner tube plays the major contribution. Overall, CFDST sections under the fire condition has a better performance.

3.3.3   Effect of interface types

Figure 5 also shows the load versus displacement curve comparison between bonded sections and non-bonded sections. The heating time for non-bonded sections are 3000s. For CFT sections, the cohesive properties have great impact during the heat treatment. Without cohesive properties, the elastic modulus of the section and max loading are much smaller. Because after increasing the temperature, the steel will lose most of the strength. Also, a gap will be produced at the interface. Hence, the overall confinement will be decreased dramatically. Furthermore, the buckle effect occurred at the top surface
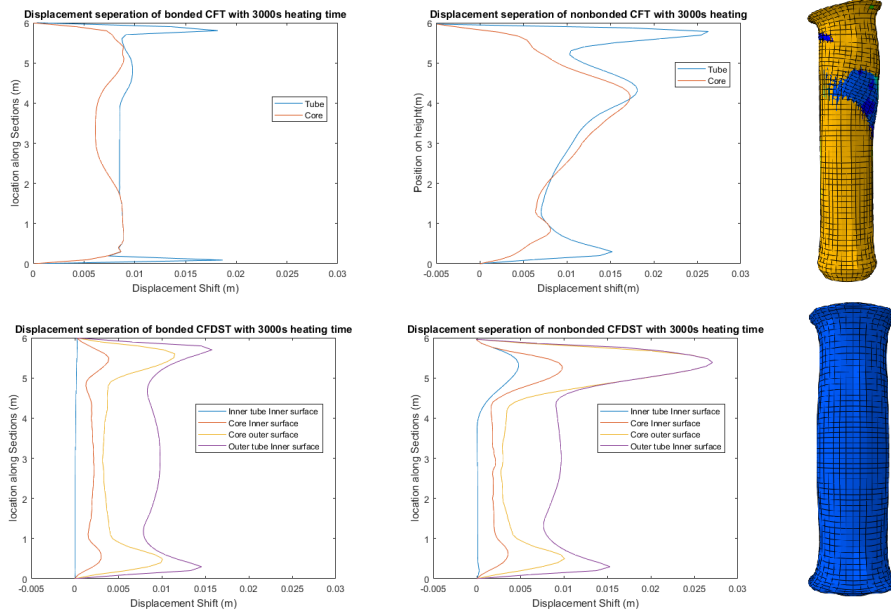
10

Figure 6: Displacement seperation

of nonbonded CFT section in Figure 6. The loading capacity of the bonded CFT section is much higher than that of the nonbonded section.

4   Conclusion

Composite sections became more and more popular especially as a foundation in the high-rise building, as their strong loading capacity. Influenced factors, which are heating time, composite section types and interface types, has been evaluated under the fire condition. These simulations have investigated the bond behaviour between steel tubes and concrete cores in composite sections. Based on the simulated results reported in this paper. The fire exposure has massive impact on the initial slope and maximum loading capacity of the displacement-load curve and displacement shift at the interface of composite sections. The following conclusions can be drawn:

1. The heating time has a significant impact on the temperature during a fire condition. It will have enormous influence on the loading capacity. It is found that the loading capacity would decrease about 50% when the heating time increases to 1000°C.

2. The interface property has great impact on the bond strength. The bond strength of bonded sections has effectively improved fire resistance. Even though the fire condition will weak the chemical bond at the interface. These simulated results are known to maintain a few bond strengths during the fire condition.

3. The Finite Element Method has the advantage of expressing the fire behaviour of composite sections under a axial compression. The comparisons of simulation results have clearly indicated the differences.

4. From mechanical point of view, a CFDST section has better performance under a fire condition. It benefits from the behaviour of inner tube. The inner tube will improve the confinement at the internal interface. Hence, the loading capacity has delight results for CFDST sections.

References

[1] Simulia, D. S. (2013). ABAQUS 6.13 User's manual. *Dassault Systems, Providence, RI.*

[2] ISO 834-1 (1999), Fire resistance tests - elements of building construction - Part 1: general requirements, *International Standard ISO 834*, Geneva.

[3] Zhao, X. L., & Han, L. H. (2006). Double skin composite construction. *Progress in structural engineering and materials*, 8(3), 93-102.

[4] Huang, H., Han, L.H., Tao, Z., & Zhao, X. L. (2010). Analytical behaviour of concrete-filled double skin steel tubular (CFDST) stub columns. *Journal of Constructional Steel Research*, 66(4), 542-555.

[5] Han, L. H., Tao, Z., Huang, H., & Zhao, X. L. (2004). Concrete-filled double skin (SHS outer and CHS inner) steel tubular beam-columns. *Thin-walled structures*, 42(9), 1329-1355.

[6] Song, T. Y., Tao, Z., Han, L. H., & Uy, B. (2017). Bond Behavior of Concrete-Filled Steel Tubes at Elevated Temperatures. *Journal of Structural Engineering*, 143(11), 04017147.

[7] Tao, Z., Han, L. H., Uy, B., & Chen, X. (2011). Post-fire bond between the steel tube and concrete in concrete-filled steel tubular columns. *Journal of Constructional Steel Research*, 67(3), 484-496.

[8] Han, L. H., & Huo, J. S. (2003). Concrete-filled hollow structural steel columns after exposure to ISO-834 fire standard. *Journal of Structural Engineering*, 129(1), 68-78.

[9] Roeder, C. W., Cameron, B., & Brown, C. B. (1999). Composite action in concrete filled tubes. *Journal of structural engineering*, 125(5), 477-484.

[10] Ma, Q., Guo, R., Zhao, Z., Lin, Z., & He, K. (2015). Mechanical properties of concrete at high temperature—a review. *Construction and Building Materials*, 93, 371-383.

[11] Li, G., & Wang, P. (2013). *Advanced analysis and design for fire safety of steel structures.* Springer Science & Business Media.